

Nature of the phase transition in compact QED

Gyan Bhanot*

Physics Department, Brookhaven National Laboratory, Upton, New York 11973

(Received 3 March 1981)

The four-dimensional O(2) gauge theory is studied by computer simulations and its phase structure is investigated by three methods: (i) by accurately measuring the action per plaquette on a 12^4 lattice, (ii) through a scaling analysis of a certain function of Wilson loops, and (iii) via its string tension. All these methods consistently indicate that the theory has a line of fixed points. The end point of this line exhibits a power-law divergence of the correlation length with index $\nu = 0.35 \pm 0.05$.

Four-dimensional compact lattice quantum electrodynamics (QED) [O(2) gauge theory] is known to have a phase transition at finite coupling.¹ To understand the continuum limit of this theory, it is necessary to understand the nature of this transition. This has proven to be quite elusive. The Migdal-Kadanoff recursion relations² suggest that the four-dimensional O(2) gauge theory is similar to the two-dimensional XY model in which the correlation length diverges exponentially at the critical point.³ The critical behavior of the XY model is understood in terms of the unbinding of vortex pairs as the temperature increases beyond criticality.⁴ In four dimensions, the analogues of vortices are strings of monopole current. Indeed, in a computer study DeGrand and Toussaint⁵ have observed the unbinding of monopole strings in the O(2) gauge theory as the bare coupling grows beyond a critical value. This tends to strengthen the Migdal-Kadanoff analogy.

On the other hand, Lautrup and Nausenberg⁶ have measured a critical finite-size scaling of the specific heat in this model, indicative of a second-order transition. Their analysis points to a power-law divergence of the correlation length with exponent $\nu = \frac{1}{3}$. Renormalization-group analyses by Hamber¹¹ also suggest an index $\nu = 0.4$.

This paper reports on a further study of the O(2) gauge theory via computer simulations. The correlation index ν was measured using three different methods.

First, the dependence of P , the average action per plaquette, on the bare coupling, in the region of the critical point, was determined accurately by long, high-statistics simulation on a 12^4 lattice. A least-squares fit to this data in the critical region gave $\nu = 0.33 \pm 0.07$ in agreement with the results of the study by Lautrup and Nausenberg.⁶

Next, following a recent suggestion of Creutz,⁷ a scaling analysis was performed in the critical region on a certain function of Wilson loops (to be defined later). Using the assumption of a

single relevant length scale and the standard arguments of scaling theory, this analysis gave $\nu = 0.37 \pm 0.03$.

Further, the inverse square of the correlation length was directly obtained by measuring the string tension (or the coefficient of the area term in the Wilson loop) of the theory. The data indicate a power-law zero in κ with exponent $2\nu = 0.78 \pm 0.10$.

Finally, using a certain renormalization scheme (to be defined) the ratio of the renormalized coupling $g_R^2(d)$ at distance scale d to the bare coupling g_0^2 was measured in the Coulomb phase of the theory. $g_R^2(d)$ was found to become independent of d for all $g_0^2 < g_{0c}^2$. As $g_0^2 \rightarrow g_{0c}^2$, $g_R^2(d)$ becomes very large and at $g_0^2 = g_{0c}^2$, g_R^2 may well be infinite. The next three sections present our study in more detail.

THE MODEL AND SIMULATION PROCEDURE

The partition function Z and the free-energy density F for the lattice theory is defined in the standard way as

$$Z(g_0^2) = \sum_{\theta} \exp\left(\frac{1}{g_0^2} \sum_p \cos\theta_p\right) = \exp[NF(g_0^2)], \quad (1)$$

where N is the number of plaquettes.

The variables θ of the theory occupy links on a hypercubical lattice and θ_p is the usual oriented sum of θ 's around a unit plaquette p . We take the θ 's to be elements of the group $Z(8)$, a subgroup of O(2). It is known that the $Z(8)$ theory has two transitions.^{1,8} One of these is a "freezing" transition near $g_0^2 \sim 0.4$ from the discrete nature of $Z(8)$. The other, near $g_0^2 \sim 1$, is the true O(2) transition.

Recent studies⁹ of the gauge theory defined on certain discrete non-Abelian subgroups of SU(2) have shown that for all couplings larger than the critical coupling of the freezing transition, these theories are, for all practical purposes, identical

to SU(2). This is intuitively sensible since the discrete nature of the group should be unimportant once the temperature is greater than the largest entropy gap. Hence, one expects the $Z(8)$ theory to be a good approximation to the $O(2)$ theory for $g_0^2 > 0.4$.

From a computational point of view, the advantage of using $Z(8)$ instead of $O(2)$ is that more than one link variable may be stored in each computer word and several variables may be processed simultaneously in a Monte Carlo iteration.¹⁰ In the present analysis a lattice of 12^4 sites was used and the entire time dimension was stored in one computer word. This reduced the effective dimension (as far as computer time was concerned) from 4 to about 3.2.

Using four hits per link and the Metropolis algorithm to bring the system to equilibrium, the CPU time for one upgrade (iteration) of the 82 944 link variables on a CDC-7600 computer was about 2 seconds.

THE AVERAGE ACTION PER PLAQUETTE

The average action per plaquette is given by

$$P = \frac{1}{N} \frac{\partial \ln Z}{\partial (1/g_0^2)} = \frac{\partial F}{\partial (1/g_0^2)} = \langle \cos \theta_p \rangle. \quad (2)$$

In the neighborhood of the $O(2)$ critical point, P varies rapidly with g_0^2 . Hence, it is advantageous to bring the lattice to equilibrium at any desired value \bar{P} of P by changing the inverse coupling $\beta = 1/g_0^2$ after each upgrade to a new value

$$\beta_{\text{new}} = \beta_{\text{old}} + 0.25(\bar{P} - P_{\text{obs}}), \quad (3)$$

where P_{obs} is the value of P measured after the upgrading. This procedure results in very rapid convergence to equilibrium even near the critical point. This method is analogous to the zone-refining technique used to eliminate localized

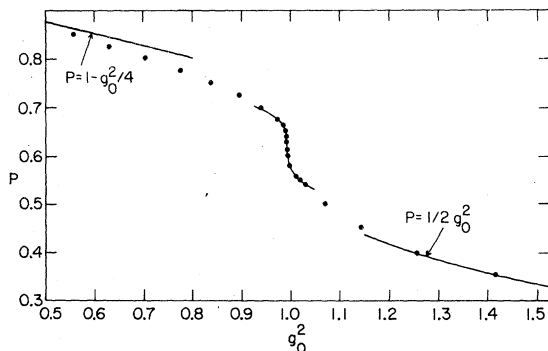


FIG. 1. Average action per plaquette versus bare coupling g_0^2 on a 12^4 lattice. The curve in the critical region is a least-squares fit which gives $\nu = 0.33$.

defects in wires by spot heating along the length of the wire causing the impurity (imperfection) to move with the heat source.

The data for P vs g_0^2 is plotted in Fig. 1. Starting at $P = 0.85$ and the lattice initially ordered, 200 upgrades were performed at each P before moving to the next. After each iteration, β was changed to a new value using Eq. (3). The statistical error on the data point in Fig. 1 is smaller than the size of the dots. The curves in Fig. 1 for large and small values of P are, respectively, the leading-order weak- and strong-coupling perturbation theory predictions. The curve in the critical region around $g_0^2 \sim 1$ is a least-squares fit to the form

$$P = P_0 + A |g_0^2 - g_{0c}^2|^\rho \epsilon(g_{0c}^2 - g_0^2), \quad (4a)$$

where $\epsilon(x)$ is ± 1 depending on whether x is positive or negative.

The best fit to the data is obtained for

$$P_0 = 0.61 \pm 0.08, \quad g_{0c}^2 = 0.997 \pm 0.010, \\ \rho = 0.33 \pm 0.27. \quad (4b)$$

The index ρ in Eq. (4a) is related to the correlation-length index ν in the following way: By the definition of ν , near g_{0c}^2 the correlation length ξ satisfies

$$\xi \sim |g_0^2 - g_{0c}^2|^{-\nu}. \quad (5)$$

The free energy density F scales similar to ξ^{-D} in D dimensions. Hence,

$$P \sim \frac{dF}{dg_0^2} \sim P_0 + |g_0^2 - g_{0c}^2|^{\nu D - 1} \Rightarrow \rho = \nu D - 1. \quad (6)$$

Using (4b), this gives $\nu = 0.33 \pm 0.07$ for $D = 4$.

SCALING ANALYSIS

An estimate of the ensemble average of planar rectangular Wilson loops $W(d, d')$, ($d, d' = 1, 6$) was obtained from the last 100 of the 200 configurations generated at each value of P . From these, the following function was constructed:

$$r(d, g_0^2) = \left[\frac{W(d, d)W(2d, 2d)}{W(d, 2d)^2} \right] \quad (7)$$

(alternately, and equivalently, r is a function of d and P).

By calculating the leading contributions to r in weak coupling, it is easy to show that the only dependence it has on the cutoff is through the bare coupling g_0^2 (or equivalently, through P). Thus r is a "physical observable." The explicit result is

$$r(d, g_0^2) \underset{g_0^2 \rightarrow 0}{\sim} \exp(-0.066g_0^2)[1 + O(g_0^2)], \quad (8a)$$

or

$$r(d, P) \underset{P \rightarrow 1}{\sim} \exp[-0.026(1 - P)][1 + O(1 - P)]. \quad (8b)$$

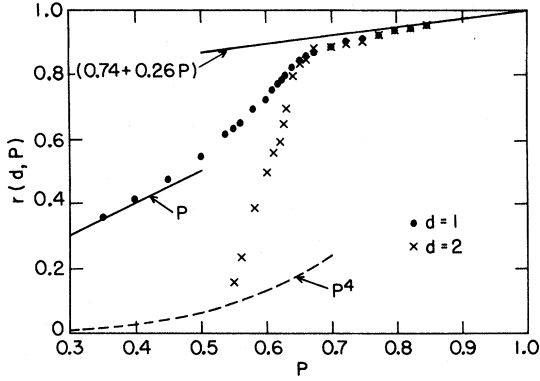


FIG. 2. $r(d, P)$ [see Eq. (7)] vs P for $d=1, 2$. The theory becomes scale invariant when the curves for $d=1$ and $d=2$ merge. A scaling analysis of the curves indicates $\nu = 0.37 \pm 0.03$.

Notice that r is also independent of d in this limit (weakly coupled QED scales).

Figure 2 is a plot of the data for r vs P for $d=1$ and $d=2$. The smooth curves in the figure are the leading-order strong- and weak-coupling estimates.

It is clear from Fig. 2 that r is independent of d for $P \geq P_0 \approx 0.65$. In other words, from the point where the curves for $d=1$ and 2 merge, the theory is scale invariant.

Under the assumption that there is a single relevant length scale ξ , it is possible to extract the index ν from Fig. 2. This is done as follows. Expanding $r(d, P)$ about the scale-invariant end point P_0 , to leading order in $(\frac{P}{\xi})$,

$$r(d, P, \xi) = r_0(P_0) + \left(\frac{d}{\xi}\right)^\sigma r_1(P_0). \quad (9)$$

Hence, defining

$$\phi_d = \left(\frac{dr(d, P)}{dP}\right)_{P=P_0}, \quad (10)$$

one obtains

$$\sigma = \frac{\ln(\phi_2/\phi_1)}{\ln 2}. \quad (11)$$

The index σ is related to ν as follows. When P is close to P_0 ,

$$r(d, P) = r_0(P_0) + (P - P_0)r_2(d, P_0). \quad (12)$$

Comparing (9) and (12) and using (5) and (6),

$$\xi^{-\sigma} \sim (P - P_0) \sim (\xi)^{(1-\nu D)/\nu} \quad (13)$$

or

$$\nu = 1/(D - \sigma). \quad (14)$$

The data were analyzed by making quadratic, cubic, and quartic polynomial fits in P to $r(d, P)$

using P values in the interval $[0.6, 0.675]$. From these fits, σ was obtained using (11). The fits were made by grouping data points into sets which approached P_0 . If ν were changing as $P \rightarrow P_0$ (characteristic of a Kosterlitz-Thouless type of singularity), one would obtain a larger value of σ from data points closer to P_0 . No such systematic trends were seen. The fits give

$$\sigma = 1.3 \pm 0.2, \quad \nu = 0.37 \pm 0.03, \quad (15)$$

$$P_0 = 0.66 \pm 0.03.$$

Creutz⁷ has recently also measured the function $r(d, P)$ for $d=1, 2$ in this theory on a 10^4 lattice with somewhat lower statistics. He finds indications that the curves for $d=1$ and $d=2$ cross twice and interprets this as the effect of monopoles. On careful perusal, this crossing is visible in Fig. 2 also. However, the effect is clearly quite weak and analysis indicates that it depends quite strongly on the lattice size. A careful treatment of this effect should be carried out but is probably quite difficult.

Finally, the string tension κ was measured as a function of g_0^2 . To do this, a further 50 iterations at fixed g_0^2 were done on the lattices obtained after 200 iterations at fixed P . Wilson loops up to 6×6 were measured over the last 25 of these iterations. To extract κ , consider the function

$$\kappa(d, g_0^2) = -\ln \left[\frac{W(d, d)}{W(d-1, d+1)} \right] \quad (16a)$$

when

$$d \rightarrow \infty, \quad \kappa(d, g_0^2) \rightarrow \kappa(g_0^2). \quad (16b)$$

Figure 3 shows the data for $\kappa(d, g_0^2)$ vs g_0^2 . It

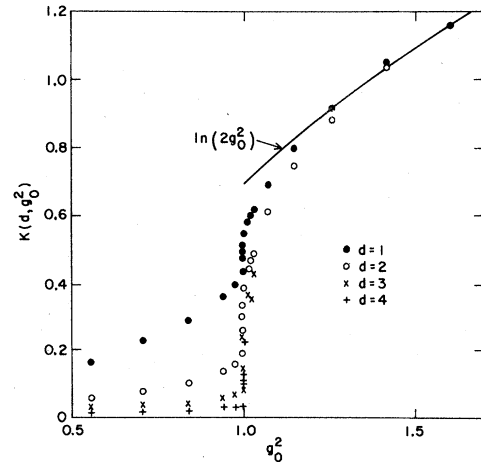


FIG. 3. $\kappa(d, g_0^2)$ vs g_0^2 for $d=1, 2, 3, 4$. In the limit $d \rightarrow \infty$, $\kappa \rightarrow$ string tension. The zero in the string tension at $g_0^2 \sim 0.99$ is clearly seen in the figure.

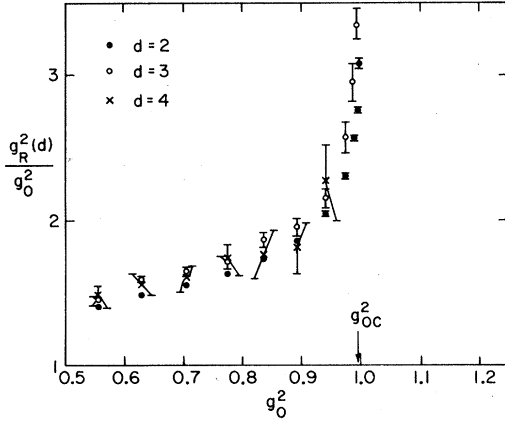


FIG. 4. $g_R^2(d)/g_0^2$ vs d for various coupling [see Eq. (17b)].

is evident that κ vanishes for $g_0^2 \leq g_{0c}^2 \sim 0.99$. To obtain the index associated with the vanishing of κ requires the following observation. As $g_0^2 \rightarrow 0$, a simple calculation shows that

$$(d^2 - 1)\kappa(d, g_0^2) \sim g_0^2 \left(\frac{1 + \pi}{\pi^2} \right) [1 + O(g_0^2)], \quad (17a)$$

which suggests that $(d^2 - 1)\kappa(d, g_0^2)$ becomes independent of d as the theory approaches scale invariance.

Indeed one may use Eq. (17) to define a renormalized coupling at the scale d . Thus, define

$$g_R^2(d) = \frac{\pi^2}{(1 + \pi)} (d^2 - 1)\kappa(d, g_0^2). \quad (17b)$$

Figure 4 is a plot of $g_R^2(d)/g_0^2$ for $d=2, 3, 4$ in the Coulomb phase. The presence of a line of fixed points for $g_0^2 \leq g_{0c}^2$ is evidenced by the fact that $g_R^2(d)/g_0^2$ is independent of d . The renormalized charge at $g_0^2 = g_{0c}^2$ is very large and may even be infinite.

For $g_0^2 > g_{0c}^2$, the string tension is nonvanishing. Figure 4 suggests that, near g_{0c}^2 ,

$$\kappa(d, g_0^2) = \kappa(g_0^2) + \frac{c(g_0^2)}{(d^2 - 1)} + O\left(\frac{1}{(d^2 - 1)^2}\right) \quad (18)$$

with $\kappa(g_0^2) = 0$ for $g_0^2 = g_{0c}^2$.

If one assumes that Eq. (18) is valid, then the combination $\hat{\kappa} = [8\kappa(3) - 3\kappa(2)]/5$ is a better estimator of κ than either $\kappa(2)$ or $\kappa(3)$. In Fig. 5, $\kappa(2)$, $\kappa(3)$, and $\hat{\kappa}$ are plotted as functions of g_0^2 . A least-squares fit to $\hat{\kappa} = A|g_0^2 - g_{0c}^2|^{2\nu}$ gives

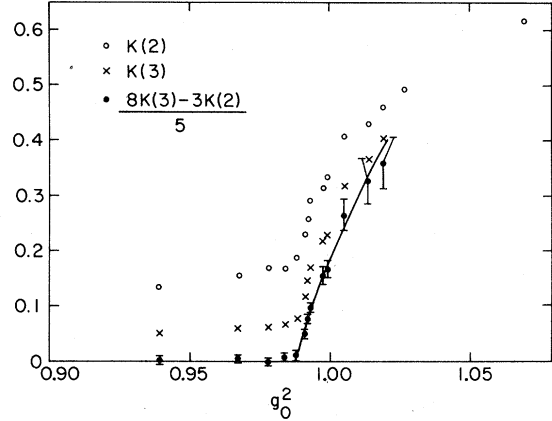


FIG. 5. String tension vs g_0^2 . The solid curve is a least-squares fit which gives $\nu = 0.39$.

$\nu = 0.39 \pm 0.05$ and $g_{0c}^2 = 0.988 \pm 0.005$. The solid curve in Fig. 5 shows this fit.

Finally, it must be stated that these data may be fit to an essential singularity. The result of such a fit is that one cannot decide between an algebraic and an essential singularity from the present data. However, the fact that the couplings of the specific heat peak and the zero in the string tension are less than one standard deviation apart, and that one gets consistently a value $\nu = 0.35 \pm 0.05$, means that the data prefers an algebraic singularity.

In summary, the present analysis of $O(2)$ gauge theory indicates that this theory has a line of fixed points along which a scale-invariant continuum limit will result. This line most probably ends in a fixed point with a power-law correlation-length divergence with index $\nu = 0.35 \pm 0.05$. This index is in agreement with specific-heat Monte Carlo results.⁶ It is also consistent with a recent block-spin renormalization-group analysis by Hamber¹¹ which gave $\nu_G = 0.4$ from the mass gap.

Note added. When this work was completed, I learned of a similar analysis of the $O(2)$ theory by DeGrand and Toussaint¹² using the Villain form of the action. Their results are more or less consistent with mine.

I thank Michael Creutz, Tom DeGrand, and Herbert Hamber for conversations. This research was supported by the U. S. Department of Energy under Contract No. DE-AC02-76CH00016.

*Address after September, 1981: Institute for Advanced Study, Princeton, NJ 08540.

- ¹M. Creutz, L. Jacobs, and C. Rebbi, Phys. Rev. Lett. 42, 1390 (1979); Phys. Rev. D 20, 1915 (1979); A. H. Guth, *ibid.* 21, 2291 (1980); T. Banks, R. Meyerson, and J. Kogut, Nucl. Phys. B129, 493 (1977).
²L. P. Kadanoff, Rev. Mod. Phys. 49, 267 (1977); A. A. Migdal, Zh. Eksp. Teor. Fiz. 69, 810 (1975) [Sov. Phys.-JETP 42, 413 (1976)].
³J. Tobochnik and G. V. Chester, Phys. Rev. B 20, 3761 (1979).
⁴J. M. Kosterlitz and D. J. Thouless, J. Phys. C 6, 1181 (1973); J. M. Kosterlitz, *ibid.* 7, 1046 (1974).
⁵T. A. DeGrand and D. Toussaint, Phys. Rev. D 22,

2478 (1980).

- ⁶B. Lautrup and M. Nauenberg, Phys. Lett. 95B, 63 (1980).
⁷M. Creutz, Phys. Rev. D 23, 1815 (1981).
⁸S. Elitzur, R. B. Pearson, and J. Shigemitsu, Phys. Rev. D 19, 3698 (1979).
⁹C. Rebbi, Phys. Rev. D 21, 3350 (1980); G. Bhanot and C. Rebbi, Nucl. Phys. B (to be published).
¹⁰L. Jacobs and C. Rebbi, Brookhaven Report No. BNL-27842, 1980 (unpublished).
¹¹H. Hamber, Phys. Rev. D (to be published).
¹²T. DeGrand and D. Toussaint, following paper, Phys. Rev. D 24, 466 (1981).